Theoretical study of the X $^1\Sigma^+$ states of the alkali hydrides NaH–CsH ⊘

Stephen R. Langhoff; Charles W. Bauschlicher, Jr.; Harry Partridge

Check for updates

View Online

Export Citation

Articles You May Be Interested In

Core–valence correlation effects using approximate operators

J. Chem. Phys. (February 1991)

On the dissociation energy of Mg_2

J. Chem. Phys. (May 1990)

An *ab initio* study of core–valence correlation

J. Chem. Phys. (August 1983)

Theoretical study of the $X \, {}^1\Sigma^+$ states of the alkali hydrides NaH–CsH

Stephen R. Langhoff and Charles W. Bauschlicher, Jr.

NASA Ames Research Center, Moffett Field, California 94035

Harry Partridge

Research Institute for Advanced Computer Science, NASA Ames Research Center, Moffett Field, California 94035

Theoretical potentials for the $X \, {}^1\Sigma^+$ states of NaH, KH, and RbH are reported using near Hartree–Fock quality Slater basis sets and incorporating electron correlation through the coupled-pair formalism (CPF). Excellent agreement is obtained with the available RKR potentials even though the CPF formalism is based on the SCF reference that dissociates incorrectly. Electric dipole moment functions are reported for NaH–RbH, as well as vibrationally averaged dipole moments, Einstein coefficients, and radiative lifetimes for the first ten vibrational levels. For KH, an extensive study is made of the computational requirements of obtaining an accurate permanent dipole moment. For CsH, r_e, ω_e, D_e, and μ_e are determined.

I. INTRODUCTION

The $X \, {}^1\Sigma^+$ ground states of the alkali hydride molecules are characterized by relatively deep potential wells arising from the $H^- + Alk^+$ ion-pair interaction. The ionic–covalent avoided crossing that occurs between the $X \, {}^1\Sigma^+$ and $A \, {}^1\Sigma^+$ potential curves gives a characteristic shape common to the family of alkali–metal hydrides.[1] This avoided crossing makes it difficult to determine accurate dissociation energies from Birge–Sponer extrapolations.[2] However, the dissociation energies of LiH,[3,4] KH,[5] and CsH[6] have been determined accurately by direct observation of energy levels near the dissociation limit. RKR potential curves have been determined[5,7–12] for at least limited portions of the $X \, {}^1\Sigma^+$ states of all of the alkali hydrides.

The 1-0 and 2-1 bands in the infrared spectrum of KH have been observed[13] at high resolution using a diode laser based spectrometer, thereby permitting an accurate determination of the equilibrium bond length. The infrared spectrum of LiH has also been reported.[14] However, these experiments give no information regarding the band strengths of the infrared vibrational–rotational bands. Permanent dipole moments have been measured only for the $v = 0$–2 vibrational levels of LiH,[15] and for the $v = 0$ level of NaH.[16]

The alkali atoms and alkali hydrides have been important systems for theoretical studies of core-valence (CV) correlation[17,18] and the development of pseudopotential methods.[19–21] Accurate theoretical potentials and radiative transition probabilities have been obtained for the $X \, {}^1\Sigma^+$, $A \, {}^1\Sigma^+$, and $B \, {}^1\Pi$ states of LiH.[22–24] Accurate theoretical potentials are also available for the ground-and low-lying states of NaH.[25,26] Recently, Zemke *et al.*[8] presented radiative transition probabilities for all vibrational levels in the $X \, {}^1\Sigma^+$ state of NaH based on an electric dipole moment function $\mu(r)$ derived from the CV wave functions of Olson and Liu.[26] However, comparatively little is known of the $\mu(r)$ and radiative lifetimes in the $X \, {}^1\Sigma^+$ states of the heavier alkali hydrides KH through CsH.

In this work we present accurate potential energy curves, $\mu(r)$ and dipole moment expectation values for the $X \, {}^1\Sigma^+$

states of NaH, KH, and RbH. More limited results $(r_e, \omega_e, D_e, \mu_e)$ are also given for CsH. Near Hartree-Fock quality Slater basis sets are employed and electron correlation is incorporated with the coupled-pair functional (CPF) formalism[27] correlating the outermost 10 valence electrons. Comparison with the available RKR potentials indicates that the CPF method gives remarkably accurate potentials even though the method is based on an SCF reference that dissociates incorrectly. The CPF $\mu(r)$ for NaH is in excellent agreement with the CV $\mu(r)$ of Olson and Liu,[26] and it is expected that the results reported here for the heavier alkali hydrides are also very accurate.

In Sec. II we discuss the computational requirements for obtaining accurate potentials and $\mu(r)$. In particular, for KH we compare the spectroscopic parameters and dipole moments derived from multireference CV and SDCI methods with those derived from CPF methods. In Sec. III we compare the theoretical spectroscopic parameters with experiment. In Sec. IV we present dipole moment matrix elements, Einstein coefficients, and vibrational lifetimes for NaH–RbH. Sec. V contains our conclusions.

II. METHODS

Extended Slater basis sets have been used for all of the alkali metals considered in the present study. Beginning with the accurate sets of Clementi and Roetti,[28] the basis sets were first modified slightly to reduce linear dependency and then augmented with diffuse and polarization functions. The basis sets are explicitly given in Table I. The metal atom basis sets are double-zeta in the core, but contain a more accurate description of the valence electrons. Since we are correlating the $(n\text{-}1)$ shell in this work, tight d functions are necessary to obtain a substantial portion of the correlation energy and to avoid basis set superposition errors. Also, since the alkali atom ${}^2S$ and ${}^2P$ states are very diffuse, s and p functions are also required on the metal atoms to avoid superposition errors that can artificially increase D_e. The difference between our SCF energies and numerical Hartree–Fock are 0.005 eV for Na and K, 0.28 eV for Rb and 0.48 eV for Cs. However,

TABLE I. Slater basis sets.

Na basis	K basis	Rb basis	Cs basis	H basis
1s(18.704)	1s(31.525)	1s(38.058 9)	1s(56.231 412)	1s(3.883)
1s(11.153)	1s(19.135)	1s(26.178 9)	1s(37.677 605)	2s(2.18)
2s(9.990)	2s(16.498 6)	2s(17.875 9)	2s(33.000 0)	1s(1.0)
2s(4.069)	2s(7.674 1)	2s(15.137 6)	2s(23.663 798)	1s(0.5)
3s(3.081)	3s(6.685 08)	3s(9.327 26)	3s(16.001 17 9)	2p(2.324)
3s(2.1335)	3s(4.041 02)	3s(6.805 48)	3s(12.807 302)	2p(1.077)
3s(1.186)	3s(2.669 19)	4s(5.535)	4s(7.762 725)	2p(0.381)
3s(0.724)	4s(2.597 94)	4s(3.914 18)	4s(5.858 331)	3d(1.85)
2p(7.943)	4s(1.290 17)	4s(2.589 77)	5s(3.958 971)	3d(0.9)
2p(4.262)	4s(0.766 41)	5s(1.880 43)	5s(2.658 013)	
2p(2.295)	4s(0.562 03)	5s(1.154 680)	6s(2.13)	
3p(2.00)	2p(15.193 6)	5s(0.768 57)ᵃ	6s(1.51)	
3p(1.247)	2p(8.641 87)	5s(0.512)ᵃ	6s(1.068)	
3p(0.8818)	3p(6.913 59)	2p(24.463 5)	6s(0.757)	
3d(4.096)	3p(3.261 63)	2p(15.285 7)	2p(35.277 273)	
3d(2.56)	3p(2.009 84)	3p(8.244 57)	2p(23.712 551)	
3d(1.6)	3p(1.688 76)	3p(5.697 39)	3p(15.6)	
3d(1.0)	4p(1.290 2)	4p(3.643 26)	3p(10.8)	
4f(2.75)	4p(0.766 41)	4p(2.333 47)	4p(9.806 642)	
4f(1.5)	4p(0.562 03)	4p(1.565 7)	4p(6.171 388)	
	3d(5.062)	5p(1.5)	5p(4.133 844)	
	3d(3.375)	5p(1.06)	5p(2.789 953)	
	3d(2.25)	5p(0.706)ᵃ	5p(1.801 024)	
	3d(1.5)	5p(0.471)ᵃ	5p(1.2)	
	3d(1.0)	3d(12.2982)	5p(0.8)	
	4f(3.0)	3d(6.791 96)	3d(21.563 487)	
	5f(3.0)	3d(4.053 72)	3d(12.657 761)	
		4d(3.75)ᵃ	4d(8.945 584)	
		4d(2.5)	4d(6.058 925)	
		4d(1.25)	4d(3.844 229)	
		4d(0.75)	4d(2.56)	
		4f(2.75)	4d(1.71)	
		4f(1.5)	4d(1.14)	
			4d(0.76)	
			4f(2.0)	
			4f(1.0)	

ᵃ These functions were not included in the computation of the potential and EDMF, but were used to determine D_e, ω_e, and r_e.

most of the error for Rb and Cs is in the core and is not likely to significantly affect the spectroscopic parameters that are determined primarily by the valence electrons. The basis set for hydrogen in Table I is capable of describing both H and H⁻, which is a requirement owing to the significant Alk⁺H⁻ character in the wave functions. The dipole moments of the alkali hydrides are expected to be converged with respect to further extensions of the one-particle basis sets at the CPF level, based on basis set saturation tests for KH and RbH.

The valence ns electron of the alkali atoms has a radial expectation value that is much larger than the next inner shell. Since this valence ns electron is weakly bound, the small interaction with the $(n-1)$ shell electrons leads to a sizable contraction of the valence orbital and a significant effect on the molecular properties. Since this core–valence (CV) correlation energy is small relative to the core–core correlation energy, it is difficult to compute the full CV effect on the molecular properties. However, for quantitative results, especially for the heavier alkali atoms, it is necessary to include the $(n-1)$ shell in the correlation treatment. At the so-called CV level of treatment, all single and double excitations involving the valence electrons, as well as all single excitations out of the core, and the class of double excitations

with one core and one valence excitation are included. Relative to a traditional SDCI calculation, this CVCI treatment excludes the class of double excitations that involve two core electrons. The CVCI approach can overestimate the contraction effect since it excludes the core–core correlation which uses the same variational space, and it is not invariant to mixing of the core and valence orbitals. In general, however, the CV approach gives excellent results for these systems, as evidenced by the results of Olsen and Liu[26] for NaH. Müller, Flesch, and Meyer[21] have proposed an effective potential method for including the CV correlation. Since these potentials are calibrated based on experimental atomic properties they may account correctly for the core–core correlation exclusion effect. Although the SDCI energy is invariant to the choice of the core and valence orbitals, the core–core correlation is much larger than the CV correlation (30 times larger for Na), and the important differential effect of CV correlation tends to be underestimated. This problem can be alleviated by including higher excitations, either through a multireference SDCI (MRSDCI) calculation or by the CPF approach.[27] Apparently, the unlinked higher excitations included in the CPF formalism result in an accurate balance between core–valence and core–core correlation. The CPF approach also has the advantages that the dimension of the

CI expansion is equal to that of a single reference SDCI calculation, and the density matrix is corrected for the importance of the higher excitations. Thus properties are much more superior at the CPF level, unless the effects of higher excitations are incorporated into the MRSDCI approach, by, for example, evaluating the dipole moment using the finite-field approach. Hence, the CPF method is a cost-effective approach for treating these systems, and can be employed with extensive one-particle basis sets.

In the following discussion, we compare the CPF results for r_e, D_e, and ω_e of KH, with those based on multireference treatments. For the X $^1\Sigma^+$ state of KH, the SCF occupation is $\cdots6\sigma^2 2\pi^4$. This occupation dissociates to the ionic limit instead of ground-state atoms. To obtain a wave function that dissociates properly, it is necessary to correlate the bonding pair of electrons in the 6σ and 7σ orbitals. This is accomplished by performing a complete active space self-consistent field (CASSCF) calculation[29] with the K $4s$ and H $1s$ orbitals active. In addition, to account for the $4s$-$4p$ near degeneracy in K, it is necessary to include the K $4p$ shell in the active space. We denote the CASSCF calculations as CASSCF(n) where n is the number of active orbitals. More extensive correlation is included by a valence CI (VCI), which correlates only the two valence electrons, CVCI(n) calculations that include all CV excitations from the configurations with nonvanishing coefficients in the CASSCF(n) calculations, and multireference SDCI calculations, denoted SDCI(n).

In Table II we compare the spectroscopic parameters (r_e,D_e,ω_e) for the X $^1\Sigma^+$ state of KH computed using various multireference approaches with those obtained from the

CPF approach. The Slater basis sets in Table I were used, except that the K $3d$(1.0) function was not included. Also, the potassium $3s$ electrons were not correlated resulting in an eight electron CI treatment. The SCF wave function does not dissociate to neutral atoms, and gives both D_e and r_e too large. The addition of the configurations that yield proper dissociation, CASSCF(2), results in a still longer bond length and a D_e that is too small. When the $4s$-$4p$ near degeneracy is accounted for by the CASSCF(5) wave function, D_e is substantially improved and the spectroscopic parameters are similar to the VCI results. However, at the VCI level, r_e is still too long by 0.08 Å. When CV correlation is added to the SCF, the bond length becomes shorter than experiment, and D_e is too large, because the CV wave function does not dissociate correctly. However, the multireference CV treatments lead to longer bond lengths and smaller D_e in much better agreement with experiment. By comparing the CVCI(1) calculations based on either the SCF or CASSCF orbitals, it is clear that much of the difference arises from a better localization of the core and valence orbitals in the CASSCF treatment. Thus, the addition of more references actually leads to a smaller D_e and a larger r_e for the CVCI(5) treatment. The CVCI results suggest that there is some core–core contribution to the dissociation energy. The SCF/SDCI potential does not dissociate to neutral atoms, and is therefore not suitable for the calculation of the spectra. The MRSDCI calculations dissociate correctly, and unlike the MRCV calculations, improving the reference space increases D_e and reduces r_e. The SDCI(5) calculation has a D_e which is slightly better than the CVCI(5) value, but the SDCI(5) r_e is 0.024 Å longer than experiment, while the CVCI value is only 0.006 Å shorter. The CPF approach yields the same D_e as the SDCI(5), but r_e is 0.009 Å shorter. If the potassium $3s$ orbital is included in the correlation treatment, r_e is further reduced by 0.005 Å, and overall the results are in good accord with experiment.

Since a principal goal of the present work was to compute accurate $\mu(r)$, we also considered the sensitivity of the permanent dipole moment of KH (at $r = 4.3$ bohr) to the level of the correlation treatment. The full basis set is used and the potassium $3s$ correlation is included. The SCF μ of 3.489 a.u. decreases slightly to 3.411 at the SDCI level. When higher excitations are included by the CPF approach μ substantially decreases to 3.196 a.u. The inclusion of CV correlation through the CVCI(5) calculation reduces μ to 3.143 a.u. This reduction is 118% of the difference between the SCF and CPF μ values, which indicates that the CVCI treatment may be overestimating slightly the CV effect. An accurate experimental value for the permanent dipole moment of KH would be valuable in establishing whether the CPF or CVCI dipole moment is more accurate. The CASSCF(5) calculation gives a μ of 3.403 a.u., which is smaller than the SDCI value. When all 10 CSFs in the CASSCF wave function are used as references in the MRSDCI calculation, μ is further reduced, becoming 3.322 a.u. If the CASSCF is further expanded to include an extra σ and π orbital, neither the CASSCF nor the MRSDCI μ values are significantly changed. Thus, the MRSDCI treatment appears to be converged with respect to further expansion of

TABLE II. Spectroscopic parameters for the X $^1\Sigma^+$ state of KH at various levels of correlation treatment.

Method[a]	r_e (Å)	D_e (eV)[b]	ω_e (cm^{-1})
SCF	2.308	3.23[c]	967
CASSCF(2)	2.346	1.38	875
CASSCF(5)	2.323	1.79	925
Valence CI	2.328	1.85	933
SCF/CV(1)	2.212	1.90[c]	1010
CASSCF(2)/CV(1)	2.236	1.97[c]	964
CASSCF(5)/CV(1)	2.241	1.96[c]	977
CASSCF(2)/CV(2)	2.237	1.79	976
CASSCF(5)/CV(5)	2.239	1.78	964
SCF/SDCI(1)	2.256	3.15[c]	985
CASSCF(2)/SDCI(2)	2.271	1.73	950
CASSCF(5)/SDCI(5)	2.269	1.80	955
SCF/CPF	2.260	1.80	943
SCF/CPF(+ 3s)[d]	2.255	1.80	948
Expt.	2.240	1.83	983.6

[a] The notation designates the number of nonzero CSFs in the CASSCF optimization and the number of reference configurations used in the correlation treatment. Eight valence electrons are correlated except where denoted (+ 3s).

[b] The dissociation energies are given with respect to the energy of the molecule at 15.0 bohr.

[c] Values are too large because the wave function dissociates incorrectly.

[d] These numbers differ slightly from the corresponding results in Table IV, since the basis did not contain the $3d$(1.0) Slater function on potassium.

the valence space, but the difference between MRSDCI and SCF is only 57% of the difference between SCF and CPF. The MRSDCI calculation appears to be limited by the fact that the CASSCF active space and MRSDCI reference space cannot be easily expanded to include the 3s and 3p orbitals. Hence, the calculation is missing the higher excitations required to balance the core–core and core–valence correlation. Since these higher excitations are included in the CPF treatment, the CPF shows a larger CV effect, but not as large as in the CVCI treatment where the balance is now in favor of the core–valence correlation.

It is clear that both the CV and SDCI treatments require a CASSCF reference. In contrast, the CPF technique yields excellent results using an SCF reference. The higher excitations included in the CPF yield a correct balance between the core–core and core–valence correlation, thus the potential and dipole moment function are expected to be among the most reliable. When this accuracy is combined with the cost, the CPF approach becomes the method of choice.

The core–valence calculations were carried out on the Cray XMP using the SWEDEN codes.[30] The SDCI and CPF calculations were carried out on the Cyber 205 using the Karlsruhe adaptation[31] of the COLUMBUS codes.[32-35] The Slater integrals were evaluated with the diatomics integral program DERIC.[36]

III. SPECTROSCOPIC CONSTANTS FOR THE ALKALI HYDRIDES

Since the X $^1\Sigma^+$ potentials are significantly influenced by the avoided crossing between the ionic and neutral asymptotes, it is relevant to consider how accurately the theoretical calculations reproduce the ionization potentials (I. P.) of the alkali atoms. In Table III we compare the I. P. of Na–Cs at the SCF, numerical Hartree–Fock (NHF), relativistic Hartree–Fock (RHF), SDCI, and CPF levels with experiment. The RHF treatment includes the mass velocity and Darwin terms. Our SCF treatment reproduces the NHF I. P. in every case. The difference between NHF and RHF is a measure of the importance of relativistic effects. Since relativistic effects are slightly larger for the neutral atoms, the I. P. of the alkali atoms are increased. The increase for Cs is about 0.12 eV, which agrees well with the increase of about 0.14 eV reported by Laskowski et al.[37] at the CI level from a comparison of nonrelativistic all-electron calculations with those using a relativistic effective core potential.

TABLE III. Ionization potentials (eV) for the alkali atoms.

Atom	Theoretical[a]					Expt.[b]
	SCF	NHF	RHF	SDCI	CPF	
Na	4.95	4.95	4.96	5.10	5.12	5.138
K	4.01	4.01	4.02	4.23	4.29	4.339
Rb	3.74	3.74	3.80	4.00	4.06	4.176
Cs	3.36	3.36	3.47	3.62	3.69	3.893

[a] The notations are SCF (self-consistent field), NHF (numerical Hartree–Fock), RHF (relativistic Hartree–Fock), SDCI (single-reference singles plus doubles configuration interaction), and CPF (coupled pair functional).
[b] Reference 42.

TABLE IV. Spectroscopic parameters for the X $^1\Sigma^+$ states of NaH–CsH.

Molecule	r_e (Å)		ω_e (cm⁻¹)		D_e (eV)	
	CPF	Expt.[a]	CPF	Expt.[a]	CPF	Expt.
NaH	1.890	1.887	1163	1172.2	1.92	1.98 ± 0.05[b]
KH	2.257	2.240[c]	968	983.6	1.79	1.832[c]
RbH	2.397	2.367	913	936.9	1.75	1.81 ± 0.07[b]
CsH	2.529	2.494	848	891.0	1.86	1.836[d]

[a] Reference 43.
[b] Reference 39.
[c] Reference 5.
[d] Reference 6.

The I. P. of all of the alkali atoms increase with the inclusion of electron correlation, and at the CPF level the I. P. of Na and K are in error by only 0.02 eV and 0.05 eV, respectively. The errors for Rb and Cs are somewhat larger, and it is likely that of the remaining 0.2 eV error in the I. P. of Cs, approximately 2/3 is from neglect of relativistic effects as compared to higher excitations not accounted for in the CPF formalism.

The spectroscopic parameters (r_e, ω_e, D_e) at the CPF level are compared with experiment in Table IV. The theoretical values were determined from a parabolic fit (in $1/r$) to a 0.1 bohr grid of theoretical energies. A better comparison than ω_e are the vibrational eigenvalues given for NaH, KH, and RbH in Table V. The tendency of the CPF r_e to be slightly long increases for the heavier alkali atoms. This is attributed to a larger core–valence contraction effect not fully accounted for by the CPF formalism. The CPF D_e in Table IV were obtained as the difference between the minimum in the potential and the sum of the atoms since the CPF procedure is size consistent. All of the D_e values have been corrected for superposition errors (SE) using the counterpoise method.[38] However, these SE corrections are at most 0.03 eV. The experimental D_e in Table IV for KH and CsH are accurately known and are therefore given without error bars. To our knowledge the most accurate "experimental" D_e for NaH and RbH are the estimates of Yang et al.[39] based on extrapolating the RKR curves for the A $^1\Sigma^+$ states to the ionic–covalent avoided crossing point. Our D_e for NaH is almost certainly a firm lower bound and the correct D_e is probably several hundredths of an eV larger. Hence, we agree with the value of Yang et al.,[39] but prefer a value in the lower half of the range given. The CPF value for KH is about 0.04 eV less than the accurate experimental value.[5] The slight underestimation of D_e shows up in the $\Delta G(v + 1/2)$ values for KH in Table V and is also consistent with overestimating r_e by 0.015 Å. Extension of the f basis to four 4f functions ($\alpha = 6.0, 3.0, 1.5, 1.0$) has a relatively small effect on r_e and D_e. Although part of the remaining 0.04 eV of binding energy may come from further saturation of the higher angular momentum space, it is likely that the core–core–valence triple excitations are not accounted for in the CPF formalism may account for much of the remaining difference. Our D_e for RbH, which is expected to be a lower bound for the same reasons as for KH, is also consistent with the estimate of Yang et al.[39] In fact, their estimate of 1.81 eV is likely quite accurate. However, it is somewhat surprising

TABLE V. Comparison of $\Delta G(v + 1/2)$ values (cm^{-1}) for the $^1\Sigma^+$ states of NaH, KH, and RbH.

	NaH			KH		RbH	
v	This work	Olson–Liu[a]	Expt.[b]	This work	Expt.[c]	This work	Expt.[d]
0	1132.3	1132.6	1132.8	944.9	955.9	885.8	909.1
1	1094.9	1094.0	1094.9	915.2	926.1	859.9	881.4
2	1057.5	1055.8	1057.7	886.0	896.9	834.7	854.1
3	1021.0	1018.3	1021.0	857.6	868.3	809.4	827.2
4	984.9	981.1	984.7	829.3	840.2	785.0	800.7
5	949.4	944.2	948.7	801.5	812.5	760.7	774.7
6	913.8	907.6	912.8	774.5	785.3	736.6	749.0
7	878.1	870.7		747.5	758.4	713.4	723.8
8	841.7	833.7		720.9	731.7	688.2	699.0

[a] Reference 26.
[b] Reference 44.
[c] Reference 5.
[d] Reference 11.

that our SE corrected D_e for CsH is slightly larger than the accurate experimental value.[6] The most likely explanation for this is that part of the 0.2 eV error in the I. P. of Cs translates into D_e. For ionic systems the error in the dissociation energy to the covalent limit is related to the error in the computed I. P. and electron affinity (EA). Since the EA of hydrogen is accurately computed, the error in D_e is directly related to the error in the I. P. of Cs. In other words, if the ionic curve is too low with respect to the neutral curve, D_e

can be artificially increased. However, since CsH is far from 100% ionic, not all of the error in the I. P. shows up in D_e.

The CPF potential and $\mu(r)$ are tabulated for the alkali hydrides in Tables VI and VII, respectively. The CPF potential for NaH is virtually identical to the RKR potential. The CPF $\Delta G(v + 1/2)$ values in Table V agree to within 1 cm^{-1} with the experimentally observed ones. The results based on the CV wave function of Olsen and Liu[26] are not quite as good since their treatment underestimates D_e by about 0.05

TABLE VI. Coupled pair functional potential energy functions for the $^1\Sigma^+$ states of NaH, KH, and RbH.[a]

R(bohr)	NaH	KH	RbH
2.00	177.211		
2.25	104.573		
2.50	57.484	148.898	
2.75	28.392	94.904	
3.00	11.621	57.200	83.580
3.25	3.131	31.856	50.788
3.50	0.131	15.687	28.622
3.60	0.020		
3.70	0.386		
3.75		6.183	14.336
4.00	3.613	1.430	5.809
4.20	6.979	0.078	2.041
4.30		0.021	
4.40		0.300	0.292
4.50	13.049	0.864	0.017
4.60			0.070
4.70	17.459	2.686	
4.80			0.991
5.00	24.242	6.647	2.754
5.50	35.223	14.979	9.435
6.00	45.047	23.949	17.625
6.50	53.240	32.614	26.062
7.00	59.591	40.495	34.112
7.50	64.140	47.322	41.464
8.00	67.173	52.912	47.953
9.00		60.213	57.888
10.0	71.485	63.572	63.677
12.0		65.649	68.081
15.0	72.385	66.245	69.711

[a] The energies are given in millihartrees relative to the computed minimum. The spectroscopic parameters and $\Delta G(v + 1/2)$ values derived from these potentials are compared with experiment in Tables IV and V, respectively.

TABLE VII. Electric dipole moment functions (a.u.) at the coupled pair functional level for the $^1\Sigma^+$ states of NaH–CsH.

R(bohr)	NaH	KH	RbH	CsH
2.00	1.6416			
2.25	1.8179			
2.50	1.9647	1.6423		
2.75	2.0974	1.9611		
3.00	2.2242	2.2175	1.8454	
3.25	2.3486	2.4397	2.1593	
3.50	2.4724	2.6349	2.4294	
3.60	2.5208			
3.70	2.5688			
3.75		2.8206	2.6715	
4.00	2.7063	2.9925	2.8909	
4.20	2.7932	3.1303	3.0568	
4.30		3.1964		
4.40		3.2616	3.2155[a]	
4.50	2.9107	3.3222	3.2926[a]	
4.60			3.3683[a]	
4.70	2.9774	3.4474		3.3237
4.80			3.5158	3.4220
4.90				3.5179
5.00	3.0540	3.6268	3.6587	
5.50	3.0945	3.8948	3.9937	
6.00	2.9811	4.1032	4.2921	
6.50	2.6693	4.2167	4.5354	
7.00	2.1743	4.1809	4.6888	
7.50	1.6019	3.9386	4.7248	
8.00	1.0920	3.4146	4.5762	
9.00		1.9533	3.5772	
10.0	0.1622	0.8974	2.1269	
12.0		0.1809	0.6073	
15.0	−0.0201	−0.0152	0.1068	

[a] With the augmented RbH basis (see Table I), the dipole moments at 4.40, 4.50, and 4.60 bohr are 3.2145, 3.2914, and 3.3670, respectively.

TABLE VIII. Expectation values μ_v of the dipole moment function and lifetimes τ_v for the first ten vibrational levels of the $X\ ^1\Sigma^+$ states of NaH, KH, and RbH.[a]

	NaH		KH		RbH	
v	μ_v (a.u.)	τ_v (ms)	μ_v (a.u.)	τ_v (ms)	μ_v (a.u.)	τ_v (ms)
0	2.5278[b]	...	3.2011	...	3.3495	...
1	2.5690	27.34	3.2584	21.62	3.4148	18.65
2	2.6094	14.59	3.3171	11.29	3.4801	9.70
3	2.6477	10.41	3.3740	7.97	3.5457	6.74
4	2.6840	8.36	3.4297	6.29	3.6115	5.27
5	2.7170	7.15	3.4836	5.30	3.6762	4.40
6	2.7459	6.35	3.5347	4.65	3.7394	3.82
7	2.7694	5.78	3.5826	4.20	3.7998	3.42
8	2.7858	5.33	3.6255	3.87	3.8570	3.13
9	2.7934	4.96	3.6619	3.61	3.9103	2.91

[a] Lifetimes for $J' = 0$ are computed from the reciprocals of the Einstein coefficients in Eq. (4). These lifetimes are probably accurate to about 5%.
[b] Experimental value is 2.52 ± 0.028 a.u. (Ref. 16).

eV. The theoretical vibrational eigenvalues contain several tenths of a cm^{-1} uncertainty owing to the limitations of the spline fit to the grid of theoretical energies. The CPF $\mu(r)$ is also virtually indistinguishable from the published results of Zemke et al.[8] based on the CV wave functions of Olsen and Liu. The resulting dipole moment matrix elements and vibrational lifetimes (see Table VIII) based on the theoretical CPF potential and $\mu(r)$ differ by only about 1% from the corrected values of Zemke et al.[8] Hence, our work supports the accuracy of their treatment for NaH. Our value also agrees within the error bounds with the experimental value reported for $v = 0$.

The CPF potential for the $X\ ^1\Sigma^+$ state of KH is compared with the recently determined RKR potential[5] in Fig. 1. If the CPF potential is shifted by -0.015 Å to bring r_e into agreement with experiment, the CPF potential maps on

FIG. 1. Comparison of the coupled pair functional potential ($\odot$) shifted by -0.015 Å with the experimentally derived RKR potential for the $X\ ^1\Sigma^+$ state of kH.
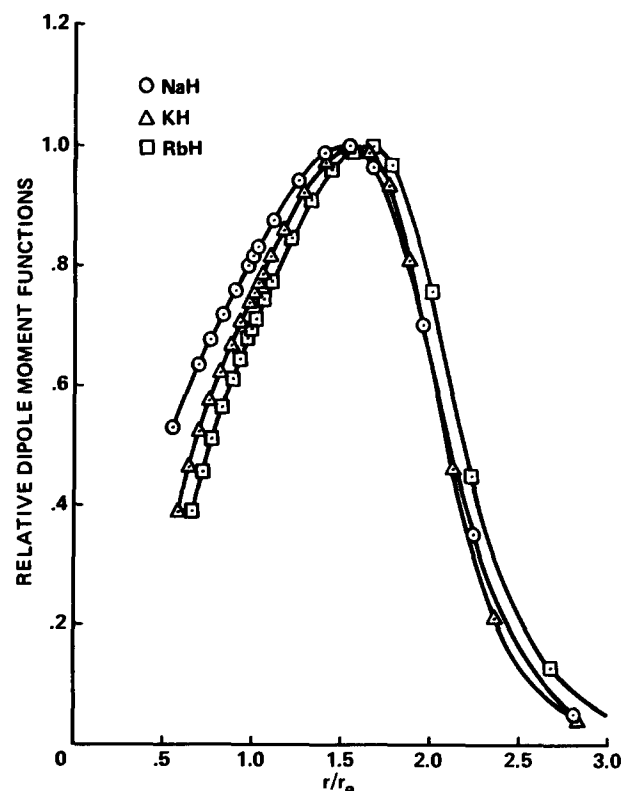

FIG. 2. Plot of $\mu(r)/\mu_{max}$ vs r/r_e for NaH, KH, and RbH where μ_{max} is the maximum in $\mu(r)$.

the RKR curve in the well region, but the underestimation of D_e by 0.03–0.04 eV can be seen at the larger r values. The underestimation of D_e also shows up in the systematically smaller $\Delta G(v + 1/2)$ values in Table V. As mentioned previously, the underestimation of D_e probably arises because the CPF formalism is not able to account for triple excitations.

A comparison of the $\mu(r)$ for the alkali hydrides show that they have the same functional form. However, the maxima occur at successively larger r values—5.41, 6.65, and 7.38 bohr for NaH, KH, and RbH, respectively. The magnitude at the maximum also increases from 3.10 a.u. for NaH to 4.22 a.u. for KH to 4.73 a.u. for RbH. In Fig. 2 we have plotted $\mu(r)/\mu_{max}$ vs r/r_e for NaH, KH, and RbH. The three curves are strikingly similar for these systems and show that simple scaling arguments can be applied to these systems with a fair degree of accuracy. This is the expected result since the characteristic functional form of $\mu(r)$ arises from the avoided crossing between the ionic and neutral curves, which occurs at larger r values as the radial extent of the alkali atom increases.

IV. VIBRATIONAL ANALYSIS OF THE THEORETICAL $\mu(r)$

In this work we have followed the approach used by Zemke et al.[8] in their treatment of NaH. In fact, we have reproduced their Table VIII exactly as a check on our implementation of the vibrational analysis. Note that the labels v' and v'' should be reversed in Table VIII of Ref. 8—see erratum. Hence, in the following discussion we give only the necessary equations to define the transition probabilities.
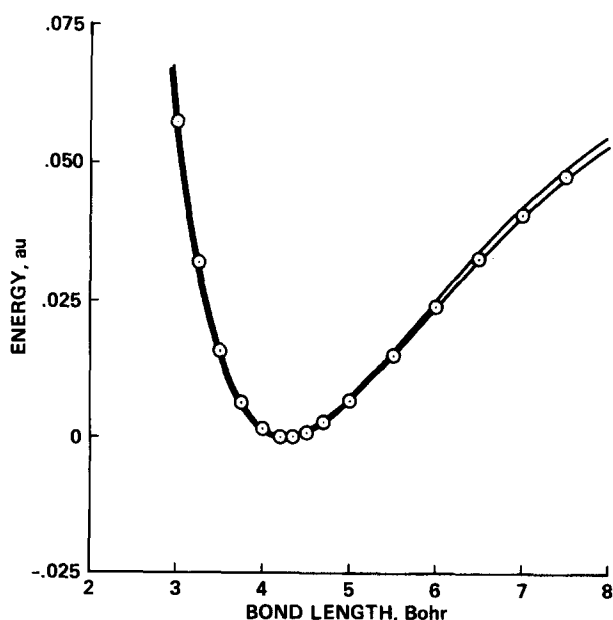
The dipole matrix elements can be written as

$$\mu_{v'J';v''J''} = \int_0^\infty \psi_{v',J'}(R)\mu(R)\psi_{v'',J''}(R)dR\,, \qquad (1)$$

where $\psi_{v',J'}$ and $\psi_{v'',J''}$ are the upper and lower normalized vibrational–rotational radial wave functions, respectively. When $v = v' = v''$ and $J = J' = J''$, we have the experimentally observable dipole moment $\mu_{v,J}$ in the v,J level.

Given the dipole moment matrix elements, the Einstein A coefficients can be written as

$$A_{v'J';v''J''}(\mathrm{s}^{-1}) = (7.2356\times10^{-6})$$

$$\times |\mu_{v'J';v''J''}|^2\, v^3_{v'J';v''J''} \quad (\mathrm{e\,\AA})^2(\mathrm{cm}^{-1})^3\,, \qquad (2)$$

where $v_{v'J';v''J''} = \mathrm{h}^{-1}(E_{v',J'} - E_{v'',J''})$ is the transition frequency. The total Einstein coefficient $A_{v',J'}$ arising from all bound–bound transitions in the $X\,^1\Sigma^+$–$X\,^1\Sigma^+$ band system is given by the expression

$$A_{v'J'} = \frac{1}{2J'+1}\left[(J')\sum_{v''}A_{v'J';v'',J'-1}\right.$$

$$\left. + (J'+1)\sum_{v''}A_{v'J';v'',J'+1}\right]. \qquad (3)$$

In this work we report values for $J' = 0$, in which case Eq. (3) reduces to

$$A_{v',0} = \sum_{v''}A_{v',0;v'',1}\,. \qquad (4)$$

The reciprocals of the $A_{v',J'}$ values are the radiative lifetimes $\tau_{v',J'}$ within the $X\,^1\Sigma^+$ manifold.

The vibrational analyses have been carried out using an extensively modified version of the diatomic intensity factor program of Zare,[40] based on the Numerov–Cooley numerical solution of the radial Schrödinger equation. Following Zemke et al.,[8] the calculations were carried out with a 0.005 Å grid from 1.0 to 13.0 Å. The vibrational eigenvalues were found to be converged with respect to the grid spacing. The range of integration is more than sufficient, especially considering that results for only the lowest ten vibrational levels are reported.

The $X\,^1\Sigma^+$ potentials for NaH, KH, and RbH consist of a spline fit to the CPF potentials in Table VI, plus an exponential term at short R defined by requiring the energy and its first derivative to match at the shortest R value computed. The ab initio potential covers a sufficiently large region of r values that it is unlikely that the results reported here for the first ten vibrational levels are affected significantly by the short range extension of the curve. In a similar fashion $\mu(r)$ is represented by a spline fit to the CPF dipole moments in Table VII. Outside this region, the dipole moment is assumed constant at the extremum values. Again, this extension of the $\mu(r)$ should not significantly affect the results since the amplitude of the first ten vibrational levels is very small in this region.

TABLE IX. Dipole moment absorption matrix elements $\mu_{v'J'=0;v''J''=1}$ (e Å units, in upper right including pure rotational transitions on the diagonal) and Einstein A spontaneous emission coefficients $A_{v'J'=0;v''J''=1}$ (in s^{-1} units, in lower left) for the $X\,^1\Sigma^+$–$X\,^1\Sigma^+$ bands in KH.[a]

	$v''(J''=1)$				
$v'(J'=0)$	0	1	2	3	4
0	1.694 02	0.085 19	− 0.010 61	0.002 02	− 0.000 41
1	4.625(+ 1)	1.724 37	0.119 82	− 0.018 08	0.003 34
2	5.287(0)	8.325(+ 1)	1.755 39	0.145 04	− 0.026 05
3	6.044(− 1)	1.396(+ 1)	1.109(+ 2)	1.785 50	0.165 49
4	5.608	1.509(0)	2.361(+ 1)	1.312(+ 2)	1.814 97
5	1.581(− 2)	2.931(− 1)	3.643(0)	4.125(+ 1)	1.436(+ 2)
6	4.345(− 2)	7.658(− 2)	8.549(− 1)	6.267(0)	5.863(+ 1)
7	5.039(− 4)	1.617(− 2)	2.068(− 1)	1.698(0)	9.790(0)
8	1.188(− 1)	2.077(− 3)	5.057(− 2)	4.498(− 1)	2.883(0)
9	2.249(− 1)	4.871(− 3)	2.065(− 2)	1.742(− 1)	1.004(0)
	5	6	7	8	9
0	− 0.000 16	0.000 21	0.000 02	− 0.000 23	0.000 27
1	− 0.000 99	0.000 37	− 0.000 13	0.000 04	− 0.000 05
2	0.005 46	− 0.001 77	0.000 64	− 0.000 25	0.000 13
3	− 0.034 26	0.007 52	− 0.002 62	0.001 10	− 0.000 48
4	0.181 86	− 0.042 95	0.009 89	− 0.003 59	0.001 56
5	1.843 50	0.194 88	− 0.052 07	0.012 39	− 0.004 59
6	1.494(+ 2)	1.870 53	0.204 49	− 0.061 72	0.015 08
7	7.783(+ 1)	1.489(+ 2)	1.895 88	0.210 66	− 0.072 16
8	1.386(+ 1)	9.856(+ 1)	1.427(+ 2)	1.918 58	0.213 04
9	4.251(0)	1.848(+ 1)	1.211(+ 2)	1.316(+ 2)	1.937 83

[a] Einstein A coefficients are in exponential notation, e.g., 4.625(+ 1) = 46.25. The dipole moment matrix elements (Einstein coefficients) are probably quite accurate for the fundamental transitions (~5%), but the uncertainly is undoubtedly larger for the higher overtones. The very high overtones ($\Delta v > 5$) are quite sensitive to the details of both the potential and the representation of the electric dipole moment function, and are thus expected to be only qualitatively correct.

TABLE X. Dipole moment absorption matrix elements $\mu_{v',J'=0;v'',J''=1}$ (e Å units, in upper right including pure rotational transitions on the diagonal) and Einstein A spontaneous emission coefficients $A_{v',J'=0;v'',J''=1}$ (in s^{-1} units, in lower left) for the $X\ ^1\Sigma^+$–$X\ ^1\Sigma^+$ bands in RbH.[a]

$v'(J'=0)$	$v''(J''=1)$				
	0	1	2	3	4
0	1.772 53	0.101 66	−0.012 51	0.002 32	−0.000 62
1	5.363(+1)	1.807 09	0.142 89	−0.021 65	0.004 53
2	6.025(0)	9.704(+1)	1.841 68	0.173 61	−0.030 74
3	6.099(−1)	1.652(+1)	1.312(+2)	1.876 37	0.198 61
4	1.055(−1)	2.297(0)	3.045(+1)	1.568(+2)	1.911 18
5	1.782(−2)	4.589(−1)	5.114(0)	4.685(+1)	1.751(+2)
6	3.010(−3)	1.104(−1)	1.188(0)	9.128(0)	6.491(+1)
7	1.120(−3)	2.793(−2)	3.231(−1)	2.455(0)	1.410(+1)
8	1.205(−3)	6.642(−3)	1.046(−1)	7.356(−1)	4.343(0)
9	1.108(−3)	2.460(−3)	3.688(−2)	2.697(−1)	1.393(0)
	5	6	7	8	9
0	0.000 19	−0.000 06	0.000 03	−0.000 03	0.000 02
1	−0.001 35	0.000 49	−0.000 19	0.000 08	−0.000 04
2	0.007 07	−0.002 27	0.000 87	−0.000 39	0.000 19
3	−0.039 91	0.009 89	−0.003 42	0.001 38	−0.000 65
4	0.219 58	−0.049 19	0.012 88	−0.004 77	0.001 99
5	1.945 41	0.237 15	−0.058 80	0.015 95	−0.006 27
6	1.863(+2)	1.978 89	0.251 83	−0.068 80	0.019 06
7	8.440(+1)	1.911(+2)	2.010 86	0.263 49	−0.079 39
8	1.964(+1)	1.049(+2)	1.900(+2)	2.041 11	0.272 01
9	6.798(0)	2.541(+1)	1.265(+2)	1.835(+2)	2.069 33

[a] See footnote a of Table IX.

Dipole matrix elements between the first ten vibrational levels in the ground state of KH are summarized in Table IX. Accurate results for higher vibrational levels could in principle be produced since the RKR curve is known to very near the dissociation limit. Following Zemke et al.,[8] Table IX is constructed with dipole matrix elements in the upper right half and on the diagonal, and Einstein A coefficients in the lower half. Since the vibrational spacing is much larger than the rotational spacing, the matrix entirely in terms of dipole matrix elements is symmetrical to within a few percent. The Einstein A coefficients in Table IX are those needed to construct the $A_{v',0}$ in Eq. (4). Overall the matrix elements are systematically larger than the corresponding values for NaH, as expected from the similar shape but larger amplitude of $\mu(r)$.

Table X contains the results of an analogous vibrational analysis for RbH. The dipole moments are uniformly slightly larger than the corresponding values for KH. This is consistent with the larger amplitude of the maximum in $\mu(r)$. The radiative lifetimes given for the first ten vibrational levels of the $X\ ^1\Sigma^+$ state of RbH in Table VIII are about 15%–20% smaller than the corresponding values for KH. The vibrationally averaged dipole moments $\langle\mu_v\rangle$ may be somewhat less accurate for RbH than for KH and NaH, because the overestimation of r_e introduces a significant difference depending on whether the RKR curve or CPF potential is used in the vibrational analysis. We have used the CPF potential here in all cases since $\mu(r)$ is derived from this wave function.

For CsH we have computed the CPF potential and $\mu(r)$ only in the vicinity of the minimum for the $X\ ^1\Sigma^+$ state. The error of 0.035 Å in the computed r_e introduces considerable uncertainty in μ_e, owing to the relatively steep ($\delta\mu/\delta r\approx 1$ a.u./bohr) slope of $\mu(r)$ in this region. Hence, μ_e is 3.498 a.u. at the theoretical r_e and 3.434 a.u. at the experimental r_e. These values are considerably smaller and probably more accurate than those reported in an earlier CI study of Laskowski and Stallcop[41] using a relativistic effective core potential. Although we have not computed dipole moment matrix elements and radiative lifetimes, from the scaling of $\mu(r)$ for NaH-RbH, we expect the dipole moment matrix elements for CsH to be larger than for RbH.

V. CONCLUSIONS

Theoretical studies of the spectroscopic parameters and dipole moment matrix elements are presented for the $X\ ^1\Sigma^+$ states of NaH through CsH. Studies of the dipole moment of KH as a function of the level of correlation treatment, show that CVCI wave functions give much better results than MRSDCI wave functions that underestimate the important CV effects. The CPF formalism, which obtains a good balance between core–core and core–valence correlation, is found to give a quantitative $\mu(r)$ even though it is based on an SCF reference that dissociates incorrectly to ions. The $\mu(r)$ are found to increase in magnitude and shift to larger r values as the radial extent of the alkali atom increases and the neutral–ionic avoided curve crossing occurs at larger r values. Hence, the intensity of the infrared spectra should

uniformly increase from NaH to CsH. The radiative lifetimes of the ground state vibrational levels, therefore, monotonically decrease for the heavier alkali atoms.

ACKNOWLEDGMENTS

[1]R. S. Mulliken, Phys. Rev. **50**, 1017, 1028 (1936).

[2]A. G. Gaydon, *Dissociation Energies and Spectra of Diatomic Molecules*, 3rd. ed. (Chapman and Hall, London, 1968).

[3]W. C. Stwalley, K. R. Way, and R. Velasco, J. Chem. Phys. **60**, 3611 (1974); C. R. Vidal and W. C. Stwalley, *ibid*. **77**, 883 (1982).

[4]K. K. Verma and W. C. Stwalley, J. Chem. Phys. **77**, 2350 (1982).

[5]K. Hussein, C. Effantin, J. D'Incan, J. Verges, and R. F. Barrow, Chem. Phys. Lett. **124**, 105 (1986).

[6]S. C. Yang, J. Chem. Phys. **77**, 2882 (1982).

[7]W. C. Stwalley, W. T. Zemke, K. R. Way, K. C. Li, and R. R. Proctor, J. Chem. Phys. **66**, 5412 (1977); **67**, 4785E (1977). See also W. T. Zemke and W. C. Stwalley, *ibid*. **68**, 4619 (1978); W. T. Zemke, K. R. Way, and W. C. Stwalley, *ibid*. **69**, 402 (1978).

[8]W. T. Zemke, R. E. Olson, K. K. Verma, W. C. Stwalley, and B. Liu, J. Chem. Phys. **80**, 356 (1984); **85**, 4209E (1986).

[9]M. Giroud and O. Nedelec, J. Chem. Phys. **73**, 4151 (1980).

[10]S. C. Yang, Y. K. Hsieh, K. K. Verma, and W. C. Stwalley, J. Mol. Spectrosc. **83**, 304 (1980).

[11]Y. K. Hsieh, S. C. Yang, A. C. Tam, K. K. Verma, and W. C. Stwalley, J. Mol. Spectrosc. **83**, 304 (1980).

[12]Y. K. Hsieh, S-C. Yang, A. C. Tam, and W. C. Stwalley, J. Chem. Phys. **68**, 1448 (1978).

[13]N. N. Haese, D-J. Liu, and R. S. Altman, J. Chem. Phys. **81**, 3766 (1984).

[14]T. C. James, W. G. Norris, and W. Klemperer, J. Chem. Phys. **32**, 728 (1960).

[15]L. Wharton, L. P. Gold, and W. Klemperer, J. Chem. Phys. **37**, 2149 (1962).

[16]P. J. Dagdigian, J. Chem. Phys. **71**, 2328 (1979).

[17]S. R. Langhoff, C. W. Bauschlicher, and H. Partridge, J. Phys. B **18**, 13 (1985).

[18]H. Partridge, C. W. Bauschlicher, S. P. Walch, and B. Liu, J. Chem. Phys. **79**, 1866 (1983).

[19]W. J. Stevens, A. M. Karo, and J. R. Hiskes, J. Chem. Phys. **74**, 3989 (1981).

[20]G. H. Jeung, J. P. Daudey, and J. P. Malrieu, J. Phys. B **16**, 699 (1983).

[21]W. Müller, J. Flesch, and W. Meyer, J. Chem. Phys. **80**, 3297 (1984).

[22]K. K. Docken and J. Hinze, J. Chem. Phys. **57**, 4928, 4936 (1972).

[23]H. Partridge and S. R. Langhoff, J. Chem. Phys. **74**, 2361 (1981).

[24]W. T. Zemke and W. C. Stwalley, J. Chem. Phys. **73**, 5584 (1980).

[25]E. S. Sachs, J. Hinze, and N. H. Sabelli, J. Chem. Phys. **62**, 3367, 3377 (1975).

[26]R. E. Olson and B. Liu, J. Chem. Phys. **73**, 2817 (1980).

[27]R. Ahlrichs, P. Scharf, and C. Ehrhardt, J. Chem. Phys. **82**, 890 (1985).

[28]E. Clementi and C. Roetti, At. Data Nucl. Data Tables **14**, 177 (1974).

[29]P. E. M. Siegbahn, A. Heiberg, B. O. Roos, and B. Levy, Phys. Scr. **21**, 323 (1980); B. O. Roos, P. R. Taylor, and P. E. M. Siegbahn, Chem. Phys. **48**, 157 (1980); P. E. M. Siegbahn, J. Almlöf, A. Heiberg, and B. O. Roos, J. Chem. Phys. **74**, 2381 (1981); B. O. Roos, Int. J. Quantum Chem. Symp. **14**, 175 (1980).

[30]SWEDEN is a vectorized SCF-MCSCF-CI program written by P. E. M. Siegbahn, C. W. Bauschlicher, B. O. Roos, P. R. Taylor, A. Heiberg, and J. Almlöf.

[31]The codes have been modified and vectorized for the Cyber 205 by R. Ahlrichs and co-workers. See also R. Ahlrichs, H.-J. Böhm, C. Ehrhardt, P. Scharf, H. Schiffer, H. Lischka, and M. Schindler, J. Comp. Chem. **6**, 200 (1985).

[32]The COLUMBUS codes include the Gaussian integral and SCF programs of R. Pitzer and the unitary group CI codes of I. Shavitt, F. Brown, H. Lischka, and R. Shepard.

[33]H. Lischka, R. Shepard, F. B. Brown, and I. Shavitt, Int. J. Quantum Chem. Symp. **15**, 91 (1981).

[34]R. M. Pitzer, J. Chem. Phys. **58**, 3111 (1973).

[35]R. Shepard, I. Shavitt, and J. Simons, J. Chem. Phys. **76**, 543 (1982).

[36]S. Hagstrom, QCPE **10**, 252 (1975); S. Hagstrom and H. Partridge (unpublished).

[37]B. C. Laskowski, S. P. Walch, and P. A. Christiansen, J. Chem. Phys. **78**, 6824 (1983).

[38]S. F. Boys and F. Bernardi, Mol. Phys. **19**, 553 (1970).

[39]S. C. Yang, D. D. Nelson, and W. C. Stwalley, J. Chem. Phys. **78**, 4541 (1983).

[40]R. N. Zare, J. Chem. Phys. **40**, 1934 (1964).

[41]B. Laskowski and J. R. Stallcop, J. Chem. Phys. **74**, 4883 (1981).

[42]C. E. Moore, Natl. Bur. Stand. (U. S.) Circ. 467 (1949).

[43]K. P. Huber and G. Herzberg, *Molecular Spectra and Molecular Structure* (Van Nostrand Reinhold, New York, 1979).

[44]F. B. Orth, W. C. Stwalley, S. C. Yang, and Y. K. Hsieh, J. Mol. Spectrosc. **79**, 314 (1980).